Model Tropical Atlantic biases underpin diminished Pacific decadal variability

Shayne McGregor[1,2]; Malte F. Stuecker[3,4]; Jules B. Kajtar[5]; Matthew H. England[2,6] and Mat Collins[5];

[1] School of Earth, Atmosphere and Environment, Monash University, Clayton, Victoria, Australia.

[2]ARC Centre of Excellence for Climate System Science, Australia
[3] Department of Atmospheric Sciences, University of Washington, Seattle, Washington, USA.
[4] Cooperative Programs for the Advancement of Earth System Science (CPAESS), University Corporation for Atmospheric Research (UCAR), Boulder, Colorado, USA.

[5] College of Engineering, Mathematics, and Physical Sciences, University of Exeter, Exeter, UK

[6] Climate Change Research Centre, University of New South Wales, Sydney, Australia

Submitted to Nature Climate Change on 14th September 2017

Pacific Trade Winds displayed unprecedented strengthening in recent decades[1]. This strengthening has been associated with east Pacific sea surface cooling[2], the early 21st Century slowdown in global surface warming[2,3], amongst a host of other substantial impacts[4-9]. Climate models fail to produce these recently observed trends[2], which is at least partly related to their underrepresentation of low frequency Pacific Ocean variability and decadal wind trends[2,10,11]. There also remains the possibility that the recent trend is a forced response that the models are misrepresenting[1,12,13]. An increasingly prominent connection between the Pacific and Atlantic basins has been highlighted as a driver of this Pacific Trade Wind strengthening[14-17] However, details of why models underestimate the magnitude of Pacific decadal trends remain unknown[2,11,16]. Here, targeted climate model experiments show that combining the recent Atlantic warming trend with the typical climate model bias leads to a substantially underestimated Pacific Ocean wind and surface temperature response. This underestimation largely stems from a reduction and eastward shift of atmospheric heating response to the tropical Atlantic warming trend. This result suggests the recent Pacific trend and model decadal variability may be better captured by models with improved climatology's.

Given the importance of the recent Pacific wind trends[2-9], it is vital to determine why climate models do not produce Pacific low frequency trade wind variability or trends of similar magnitudes to those observed. Hypotheses for the reduced decadal variability in models include some missing or misrepresented climate model dynamics (e.g., downward mixing of momentum in the atmospheric boundary layer[11]), or model mean state biases impacting Pacific trade wind variability. A recent analysis[16] suggests that mean state biases in the Atlantic appear to play a role. Here, with the aid of targeted model experiments, we seek to identify the role of common mean state biases in the Atlantic region on the representation of trans-basin variability (TBV).

Previous work utilized the Community Atmospheric Model version 4 (CAM4) to identify the prominent role of the Atlantic Ocean SST trends in forcing the intensification of tropical Pacific

Trade Winds[11]. As will be done here, the model results were compared to an ensemble of AGCM simulations forced with full observed SSTs rather than the observed trends as atmospheric models tend to underestimate the magnitude of the trade wind response (see section 2 of the Supplementary material). A series of partially coupled (PARCP) CAM4 simulations, with the observed 1992-2011 SST trend[15] prescribed over the Atlantic basin and a slab mixed layer ocean in the Pacific basin (Fig. S1; Table S1 of ref. 11), show Pacific SSTs cool in response to the remote observed Atlantic SST trend forcing. These results demonstrated that the recent Atlantic warming generates a trans-basin response, which includes a strengthening of the central Pacific wind stress (Fig. S1f) that accounts for a large portion of the strengthening found in a full SST trend forced AGCM simulation (Fig. S1c). This Pacific trade wind intensification is linked with eastern tropical Pacific cooling (Fig. S1e) that closely resembles the observations (Fig. S1a) and the negative phase of the Pacific Decadal Oscillation[16] (PDO) or the Interdecadal Pacific Oscillation[17] (IPO), which has been invoked previously as the proximate cause of the recent global warming hiatus period[2,8].

To understand the impact of model biases, a new series of CAM4 simulations, each with 5 ensemble members, is carried out. This ensemble utilises the same prescribed SST trend forcing in the Atlantic basin as described above and a slab mixed layer ocean in the Pacific basin. However, here, the ensemble mean climatological SST bias of the multi-model Coupled Model Inter-comparison Project phase 5 (CMIP5)[18] is added to the Atlantic basin such that the climatology of the Atlantic Ocean would represent the CMIP5 model average rather than the observations (Figure S2; Table S1). It is clear from the response in this simulation (Figure 1), that while the Pacific Trade Wind intensification still occurs, on average it is less than 2/3rds the

magnitude of the trend that occurs in the simulations with the observed climatology in the Atlantic Ocean (Figure 1 & S3, see Table S2). A similar under-response is found for the SST cooling trends in the eastern/central Pacific in this simulation, when compared to the experiment with prescribed observed climatology (Figure 1e, see Table S3). This change in the magnitude of the Pacific Ocean trends highlights the prominent role the background state in the Atlantic Ocean plays in the inter-basin connectivity of the model, while also raising the question of why the background state has such a pronounced impact.

In order to better understand the dynamics of how the Atlantic background state impacts the acceleration of Pacific trade winds in the absence of coupled Pacific air-sea interactions, another two sets of CAM4 simulations is carried out (10 ensemble members; Table S1). Here, the same observed 1992-2011 SST trend is applied in the Atlantic basin in each of the two-new ensemble experiments, but in contrast to the previous experiments, climatological SSTs are prescribed in the Pacific and Indian Oceans as boundary forcing (i.e. the Pacific Ocean slab mixed layer is not used) (Table S1). The difference between the two experiment sets is the Atlantic background state, as one utilises the observed while the other has the ensemble mean CMIP5 bias added.

The equatorial vertical atmospheric velocity of the AGCM simulation with observed Atlantic climatology reveals that the Atlantic basin SST trend alone leads to an upward motion (Fig. 2a) and increased precipitation (Fig. 3a) trends over most of the Atlantic region and descending drying trend elsewhere (Figure 2a, 3a and S4b). This is consistent with the circulation expected from a Matsuno-Gill response[19,20], with descending air either side of the heating anomaly (upward motion trend), which directly links SSTs in the Atlantic region with the Pacific Ocean

Walker circulation[11-13,21] (Figure 4a). Adding the CMIP5 bias to the Atlantic region acts to both, reduce ascending motion in the Atlantic region between 90°W-30°W by approximately a quarter and shift the maximum ascending motion trends eastwards (Figure 2d & e and S4b). The reduction in vertical velocity in the western/central Atlantic region in the simulation that incorporates the CMIP5 bias is consistent with i) the reduced velocity potential in the near surface layers (Figure S5a, d, & e); and ii) the reduced absolute SST of this west/central Atlantic region with the addition of the bias putting parts of the Atlantic below the threshold required for deep convection[22,23] (Figure 3a, d, & e); both of which combined lead to reduced precipitation trend as observed in these experiments (Figure 3a, d, & e and Figure 4).

In terms of the Pacific basin changes, the observed Atlantic climatology ensemble displays a clear northward migration of the eastern Pacific Inter Tropical Convergence Zone (ITCZ) in response to the Atlantic SST trend (Figure 3)[24]. The addition of the CMIP5 Atlantic bias enhances the descending motion trend in the east and west Pacific (between 120°W-80°W and 120°E-180°E, respectively), while reducing the central Pacific (between 180°E and 120°W) descending motion trend (Figure 2d & e and Figure S4), both of which are consistent with a weakening and eastward shift of the Atlantic heating anomaly (Figure S5). The CMIP5 bias induced changes in the rate of descending air are also apparent in the lower level velocity potential (Figure S6) and lead to related decreases in rainfall trends in the east and west equatorial Pacific (Figure 3e). Focusing on the ITCZ in the east Pacific, there is no sign of northward migration when the Atlantic region CMIP5 bias is present, with the region instead displaying a suppression of rainfall trends (Figure 3d). This enhances the impression that the CMIP5 bias has acted to shift the vertical velocity trends of the unbiased ensemble eastward

(Figure 4 & S5). The addition of the CMIP5 Atlantic bias also leads to Pacific Trade Wind differences that are most apparent in the decreasing south westerlies in the north-east tropical Pacific under the ITCZ (Figure S3c and d; Figure S7c and d), but also as reduced amplitude of easterly wind speeds in the western/central equatorial Pacific (Figure S3c and d; Figure S7c and d). These reductions in wind speed and precipitation in the east and west tropical Pacific, relative to the observed climatology ensemble, lead to a corresponding surface warming by, respectively, reducing surface latent heat loss to the atmosphere in each region and increasing the amount of incoming solar radiation (Figure 4; Figure S7a, d & e; Figure S8a, d & e).

The near-surface wind response in the north-east Pacific is generated as the Atlantic trend acts to increase the temperature gradient between the Pacific and Atlantic basins. Adding the CMIP5 bias in the Atlantic region does not change this inter-basin SST gradient trend, however the north-east Pacific surface wind response is significantly weaker (Figure S3). We expect that this is due to i) the reduced precipitation in the Atlantic basin with the CMIP5 biased background state leading to weaker inflows; and ii) the cooler upper atmosphere temperature trends (Figure S9), weaker upper level winds between the two basins (Figure S9) as both of these factors combine to reduce the amount of sinking air in the central Pacific.

Altering the magnitude of the Atlantic bias reveals a reduction in west Atlantic rainfall (Figure S10c, e and g) and vertical velocity trends (Figure S11c, e and g) as the bias magnitude increases. It is also clear that as the bias magnitude increases, the amount of central Pacific descending air (180^{o}E and 120^{o}W) also decreases, while the amount of descending air occurring to the east and west of this (between 120^{o}E - 180^{o}E and 120^{o}W - 80^{o}W) increases (Figure S4).

Again, these changes in vertical velocity trends are consistent with a weakening and eastward shift of Atlantic convection as the bias magnitude increases (Figure S5). The increase in the rate of descending air in east and west Pacific leads to a corresponding reduction in precipitation trends (Figure 3c, e and g) and an associated increase in the incoming solar radiation displayed in these regions (Figure S8), both of which scale with the magnitude of the Atlantic bias (Figure S12c and d). Decreases in latent heat flux loses (i.e., leading to relative SST warming) in both the north-east and west pacific regions are found as the Atlantic bias increases (Figure S7 and S12). While these latent heat flux changes are largely related to changes in wind speed, there is a role for changes in surface level specific humidity between the whole and double Atlantic bias runs (Figure S12). Clearly, both the changes in east and west surface latent heat flux and surface radiation, which act to warm the regions SSTs relative to simulation with the observed Atlantic climatology, scale with the magnitude of the Atlantic bias: That is the larger this Atlantic SST bias, the larger the cooling reduction found in the north-east and west Pacific.

When these CMIP5 bias magnitude experiments are carried out in a partially coupled setting (Table S1), the differences in Pacific region surface heat fluxes and surface radiation (Figure S7, S8 and S9) due to the addition of the CMIP5 Atlantic bias lead to substantial differences in the rates of Pacific SST cooling and trade wind intensification (Figure 5a, b, d and f). As expected, the reduction in the rate of central Pacific SST cooling increases as the Atlantic Bias increases (Figure 5c, e and g; Table S3). It is noted that neither the Pacific trade winds nor SST responses scale linearly with the magnitude of the Atlantic Ocean bias, which again hints at non-linear processes like atmospheric convection underlying the interbasin connection seen in the AGCM simulations. However, it is noted that i) there is a consistent relationship between each

simulation's TBV trend and the simulated Pacific wind trends; and ii) that the magnitude of the TBV trends decreases as the Atlantic SST bias increases (Figure S13).

These findings reveal that while the enhanced Atlantic warming since the early 1990s has contributed to an unusually rapid acceleration of the Pacific trade wind systems, this trade wind strengthening is substantially underestimated when the same warming is superimposed on the biased background state of the CMIP5 models. This underestimation largely stems from the added bias altering the regions that are above/below the threshold for convection, as it ultimately reduced and shifted eastward the atmospheric heating response to the tropical Atlantic warming trend. Despite only focusing on one decadal period in this manuscript, we can infer from these results that mean state biases apparent in the CMIP5 Atlantic region SSTs may potentially help to explain the reduced Pacific decadal variability produced in the models. This adds to an underrepresentation of the downward mixing of momentum through the atmospheric boundary layer in the models[11] and raises the further question of whether CMIP5 biases in the Pacific region act to further decouple the Pacific and Atlantic basins.

There still remains the open question of what caused the recent (1992-2011) decadal tropical Atlantic warming trend. The two possible drivers of the Atlantic trend are: i) natural internal variability; and ii) a forced response to aerosols or anthropogenic emissions. Under the hypothesis that this was primarily due to natural internal variability and given that the CMIP5 models underestimate both Pacific decadal variability, there is clear risk of false-positive detection and attribution statements as model-generated natural internal variability is used as the estimate of "noise" in detection and attribution studies. In addition, estimates of future decadal

changes in temperature (i.e. future hiatus or surge events) may be underestimated in magnitude. Under the hypothesis that the tropical Atlantic warming trends were instead forced, this means that models may underestimate a negative feedback in the system such that an Atlantic warming leads to a reduction of global warming, at least on decadal time-scales. While there has been a healthy discussion in the literature about large-scale hemispheric Atlantic SST trends[25-26], here it is unclear if the same drivers are responsible as we identify the tropical region of the Atlantic Ocean as being the most influential.

Methods

Model information

To determine the effect of the CMIP5 multi-model mean climatological bias on trans-basin variability we utilize the CAM4 AGCM in T42 horizontal resolution with 26 vertical layers[27] in a series of AGCM and partially coupled sensitivity experiments (Supplementary Table 1). For the AGCM experiments SSTs are prescribed everywhere as boundary conditions. For the partial coupled experiments CAM4 is coupled to a slab ocean model[11,28] in the Pacific Ocean and high latitudes, which includes annual mean mixed-layer depth at each spatial location and allows ocean mixed layer temperatures to adjust to anomalous atmospheric heat fluxes. The SST forcing in these experiments includes as components -- depending on the experiment -- the observed climatological SSTs[15], the observed 1992–2011 SST trend in the Atlantic Ocean[15], and different amplitude variations of the CMIP5[18] multi-model mean SST bias in the Atlantic (Fig. S2c). A detailed description of the different experiments is provided in the Supplementary Information (Table S1).

Statistics information

Statistical significance of the linear trends at each grid cell are calculated on the ensemble mean, where the F-statistic is used to determine whether the trend slope is significantly different from zero above the 95% confidence level. Significance of the differences between trends of different ensemble mean experiments are identified where there is no overlap between the 95% confidence intervals of the linear trends of the two experiments differenced. Trend 95% confidence intervals are calculated using the standard error along with a multiplier based on the inverse of the Student's T cumulative distribution function and the degrees of freedom. We note

that here we use the reduced effective degrees of freedom to take in to account the effects of autocorrelation in the time series (Wilks 1996).

References:

1. L'Heureux, M. L., Lee, S. & Lyon, B. Recent multidecadal strengthening of the Walker circulation across the tropical Pacific. *Nature Clim. Change* **3,** 571–576 (2013).

2. England, M. *et al.* Recent intensification of wind-driven circulation in the Pacific and the ongoing warming hiatus. *Nature Clim. Change* **4,** 222–227 (2014).

3. Timmermann, A., McGregor, S. & Jin, F. F. Wind effects on past and future regional sea level trends in the Southern Indo-Pacific. *J. Clim.* **23,** 4429–4437 (2010).

4. McGregor, S., Sen Gupta, A. & England, M. H. Constraining wind stress products with sea surface height observations and implications for Pacific Ocean sea level trend attribution. *J. Clim.* **25,** 8164–8176 (2012).

5. Nidheesh, A. G., Lengaigne, M., Vialard, J., Unnikrishnan, A. S. & Dayan, H. Decadal and long-term sea level variability in the tropical Indo-Pacific Ocean. *Clim. Dynam.* **41,** 381–402 (2013).

6. Han, W. *et al.* Intensification of decadal and multi-decadal sea level variability in the western tropical Pacific during recent decades. *Clim. Dynam.* http://dx.doi.org/10.1007/s00382-013-1951-1 (2013).

7. Merrifield, M. A. & Maltrud, M. E. Regional sea level trends due to a Pacific trade wind intensification. *Geophys. Res. Lett.* **38,** L21605 (2011).

8. Kosaka, Y. & Xie, S. P. Recent global-warming hiatus tied to equatorial Pacific surface cooling. *Nature* **501,** 403–407 (2013).

9. Feng, M. *et al.* The reversal of the multi-decadal trends of the equatorial Pacific easterly winds, and the Indonesian Throughflow and Leeuwin Current transports. *Geophys. Res. Lett.* **38,** L11604 (2011).

10. Kociuba, G., & Power, S. B. Inability of CMIP5 models to simulate recent strengthening of the Walker Circulation: Implications for projections. *J. Climate*, **28**, 20–35 (2015).

11. McGregor, S. *et al.* Recent Walker circulation strengthening and Pacific cooling amplified by Atlantic warming. *Nature Climate Change*, **4**, 888–892 (2014).

12. Li X, Xie S-P, Gille ST, Yoo, C. Atlantic-induced pan-tropical climate change over the past three decades. Nat Clim Chang 6:275–280 (2016).

13. Kucharski, F. *et al*. Atlantic forcing of Pacific decadal variability. *Clim. Dyn.* **46**, 2337–2351 (2016).

14. Katjar, J. B., Santoso, A., McGregor, S., M. H. England, & Baillie, Z. Model under-representation of decadal Pacific trade wind trends and its link to tropical Atlantic bias, Clim. Dyn. (2016).

15. Hansen, J., Ruedy, R., Sato, M. & Lo, K. Global surface temperature change. *Rev. Geophys.* **48,** RG4004 (2010).

16. Mantua, N. J., Hare, S. R., Zhang, Y., Wallace, J. M. & Francis, R. C. A Pacific interdecadal climate oscillation with impacts on salmon production. *Bull. Am. Meteorol. Soc.* **78,** 1069–1079 (1997).

17. Power, S., Casey, T., Folland, C., Colman, A. & Mehta, V. Inter-decadal modulation of the impact of ENSO on Australia. *Clim. Dynam.* **15,** 319–324 (1999).

18. Taylor, K. E., Stouffer, R. J. & Meehl, G. A. An overview of CMIP5 and the experiment design. *Bull. Am. Meteorol. Soc.* **93,** 485–498 (2012).

19. Matsuno T. Quasi-geostrophic motions in the equatorial area. J. Meteorol. Soc. Jpn 44: 25–43 (1966).

20. Gill, A. Some simple solutions for heat-induced tropical circulation. *Q. J. R. Meteorol. Soc.* **106,** 447–462 (1980).

21. Polo, I., Martin-Rey, M., Rodriguez-Fonseca, B., Kucharski, F. & Mechoso, C. R. Processes in the Pacific La Nina onset triggered by the Atlantic Nino. Clim Dyn. doi:10.1007/s00382-014-2354-7 (2014).

22. Graham, N. E. & Barnett, T. P. Sea surface temperature, surface wind divergence, and convection over tropical oceans. Science 238, 657–659 (1987).

23. Johnson, N. C. & Xie, S. P. Changes in the sea surface temperature threshold for tropical convection. *Nature Geosci.* **3,** 842–845, DOI: 10.1038/NGEO1008 (2010).

24. Timmermann, A. Okumura, Y., An, S.-I., Clement, A., Dong, B., Guilyardi, E., Hu, A., Jungclaus, J. H., Renold, M., Stocker, T. F., Stouffer, R. J., Sutton, R., Xie, S.-P. & Yin, J. (2007) The influence of a weakening of the Atlantic Meridional overturning circulation on ENSO. J Clim 20:4899–4919

25. Booth, B., Dunstone, N., Halloran, P., Andrews, T. & Bellouin, N. Aerosols implicated as a prime driver of twentieth-century North Atlantic climate variability. Nature 485, 534-534, doi:10.1038/nature11138 (2012).

26. Zhang, R. et al. Have Aerosols Caused the Observed Atlantic Multidecadal Variability? Journal of the Atmospheric Sciences 70, 1135-1144, doi:10.1175/JAS-D-12-0331.1 (2013).

27. Neale, R. B. *et al.* The mean climate of the Community Atmosphere Model (CAM4) in

forced SST and fully coupled experiments. *J. Clim.* **26,** 5150–5168 (2013).

28. Stuecker, M. F., Jin, F.-F., Timmermann, A. & McGregor, S. Combination mode dynamics of the anomalous northwest Pacific anticyclone. *J. Climate*, **28**, 1093–1111, doi:https://doi.org/10.1175/JCLI-D-14-00225.1 (2015).

Acknowledgements:
This work was supported by the Australian Research Council (ARC), including the ARC Centre of Excellence in Climate System Science (ARC grant CE110001028). MFS was supported by the NOAA Climate and Global Change Postdoctoral Fellowship Program, administered by UCAR's Cooperative Programs for the Advancement of Earth System Sciences (CPAESS). JBK and MC was supported by the Natural Environment Research Council (grant number NE/N005783/1). We acknowledge the World Climate Research Programme's Working Group on Coupled Modelling, which is responsible for the Coupled Model Intercomparison Project (CMIP), and we thank the climate modelling groups for producing and making their model output available. SM also thanks Dietmar Dommenget for helpful discussions during the early stages of this work.

Author Contributions:
S.M. conceived the study and wrote the initial manuscript draft. M.F.S. conducted the AGCM and partially coupled model simulations, while S.M. and J.B.K. analysed the model output and generated figures. All authors contributed to interpreting the results, discussion of the associated dynamics, and refinement of the paper.

Additional information:

Competing Financial Interests:
The authors declare no competing financial interests

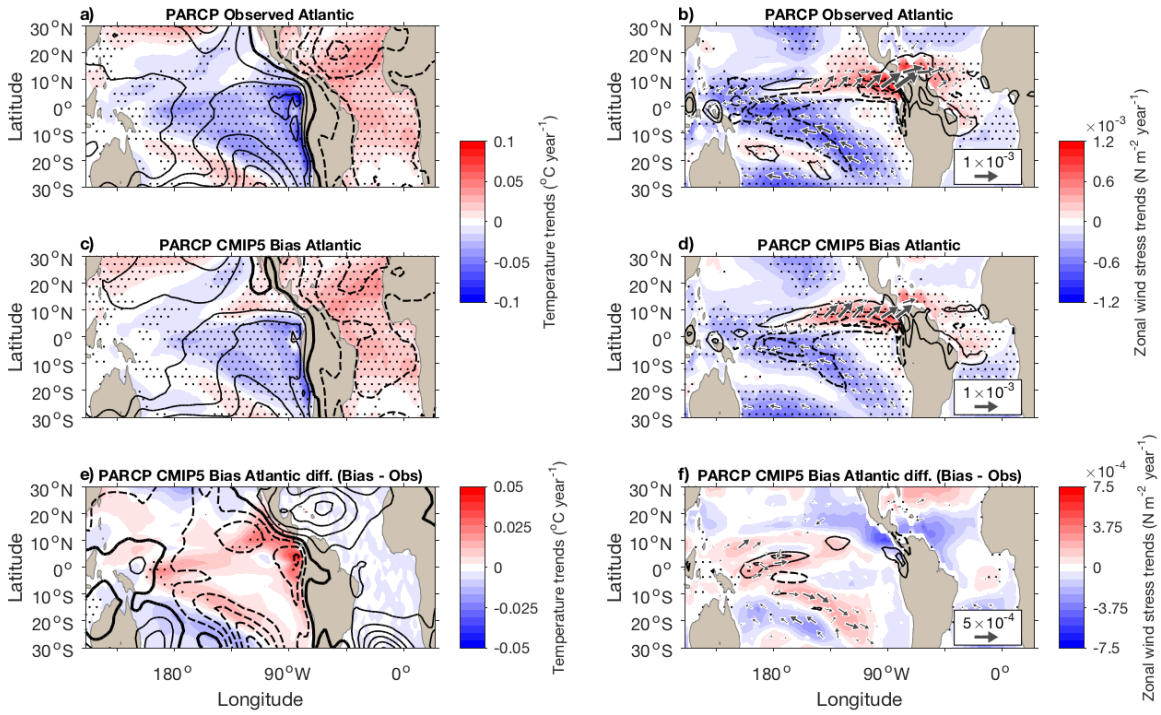

Figure 1: Trends (1992–2011) of PARCP SST, SLP, wind stress and precipitation.

a, Modelled surface temperature (shading) and SLP (contours; Pa yr^{-1}) from the partially coupled experiment forced with observed Atlantic SST trend forcing with an active Pacific mixed layer; SLP trend contours range from −15 to 15 Pa yr^{-1} with a contour level of 1.5 Pa yr^{-1}; positive contours are black, negative contours are grey, and the zero contour is a thicker black line. **b**, Modelled zonal wind stress trends (shading), significant (above the 95% level) wind stress trends (vectors), and precipitation (contours; m s^{-1} yr^{-1}) from the same experiment as presented in **a**. Precipitation trend contours shown for 0.5 and 1 x10^{-9} m s^{-1} yr^{-1} in solid black, and corresponding negative trends in dashed black. In panels **a**-**d** stippling indicates that the changes in the underlying shaded plots are significant above the 95% level. **c**,**d**, As in **a** and **b**, but for the CAM4 experiment forced with the Atlantic SST trend overlaying the *biased CMIP5 climatology* with an active Pacific mixed layer. **e** and **f** respectively presents the differences between **a** and **c**, and **b** and **d**. SLP trend difference contours range from −10 to 10 Pa yr^{-1} with a contour level of 0.5 Pa yr^{-1}. Precipitation trend difference contours shown for 2.5 and 5 x10^{-8} m s^{-1} yr^{-1} in solid black, and corresponding negative trends in dashed black. Stippling in panels **e** and **f** indicates where there is no overlap between the 95% confidence intervals of the linear trends of the two experiments differenced.

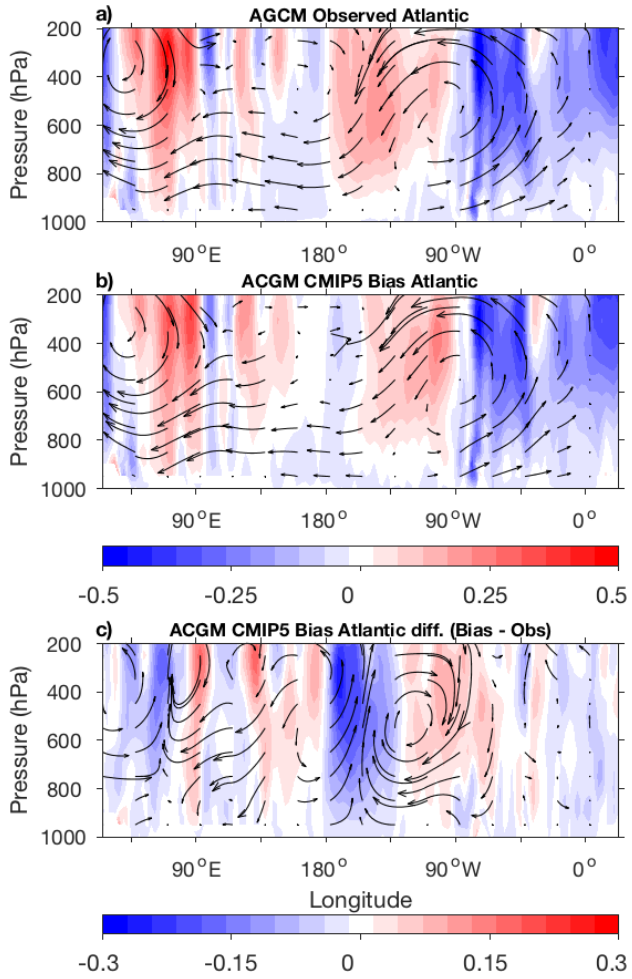

Figure 2: Changes of AGCM simulated global Walker circulation. a, Vertical equatorial (20^{o}S-20^{o}N) atmospheric velocity trends (shading) over the 1992–2011 period from the AGCM experiments forced with the Atlantic SST trend, where SSTs are set to climatology in the Pacific and Indian Oceans. Overlying vectors represent the zonal wind trend (m s^{-1} yr^{-1}) and the vertical velocity scaled by a factor of 100. **b**, As in **a**, but for the AGCM experiment forced with the same SST trend superimposed on top of the Atlantic regions observed climatology plus the whole CMIP SST bias. The difference between **b** and **a** is presented in **c**.

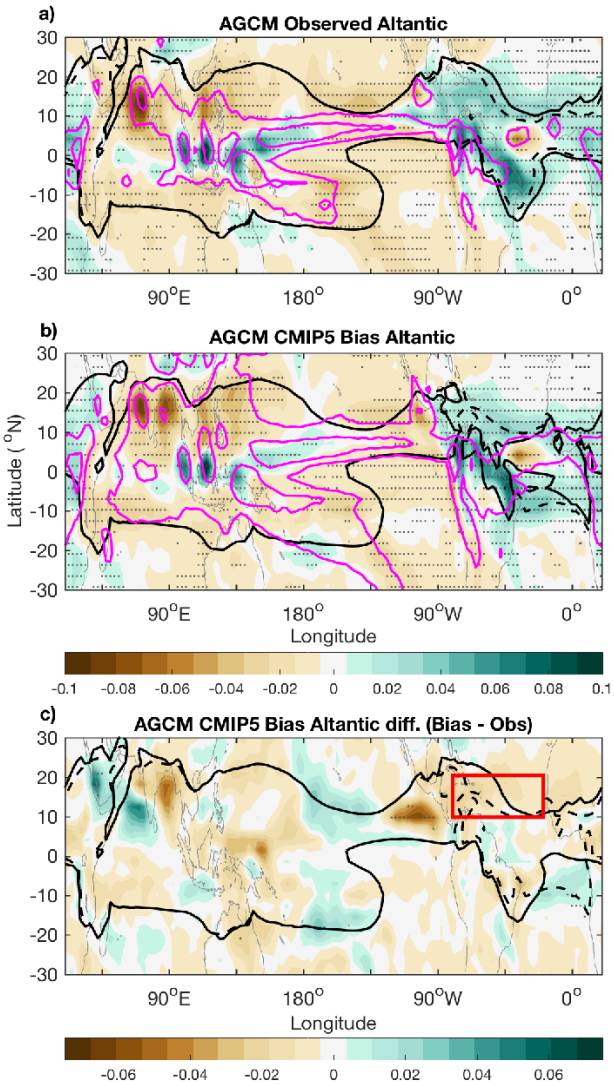

Figure 3: Changes of AGCM simulated precipitation. **a** and **b** display the ensemble average linear precipitation trends for the AGCM ensembles with Observed climatology and the CMIP5 climatology, respectively. The solid black contour in each of these panels is the climatological 27°C isotherm, while the dashed black contour in each panel is the 27°C contour after the addition of the total SST trend. The magenta contours are the mean precipitation calculated from 20-year climatologically forced simulations [6 and 9 mm/day]. Panels **c** displays the precipitation trend difference between the **b** and **a**. In this panel the black contours represent the 27°C contour after the addition of the total SST trend with the dashed contour representing the CMIP5 biased background state and the solid contour representing the 27°C the observed climatology. In panels **a** and **b** stippling indicates that the linear trends in the shaded plots are significant above the 95% level, while in panel **c** stippling indicates there is no overlap between the 95% confidence intervals of the linear trends of the two experiments differenced. It is also noted that a 2-sample T-test was utilized to show that mean precipitation trends averaged over the red boxed region (10oN-20oN and 80oW-20oW) are significantly different above the 95% confidence level.

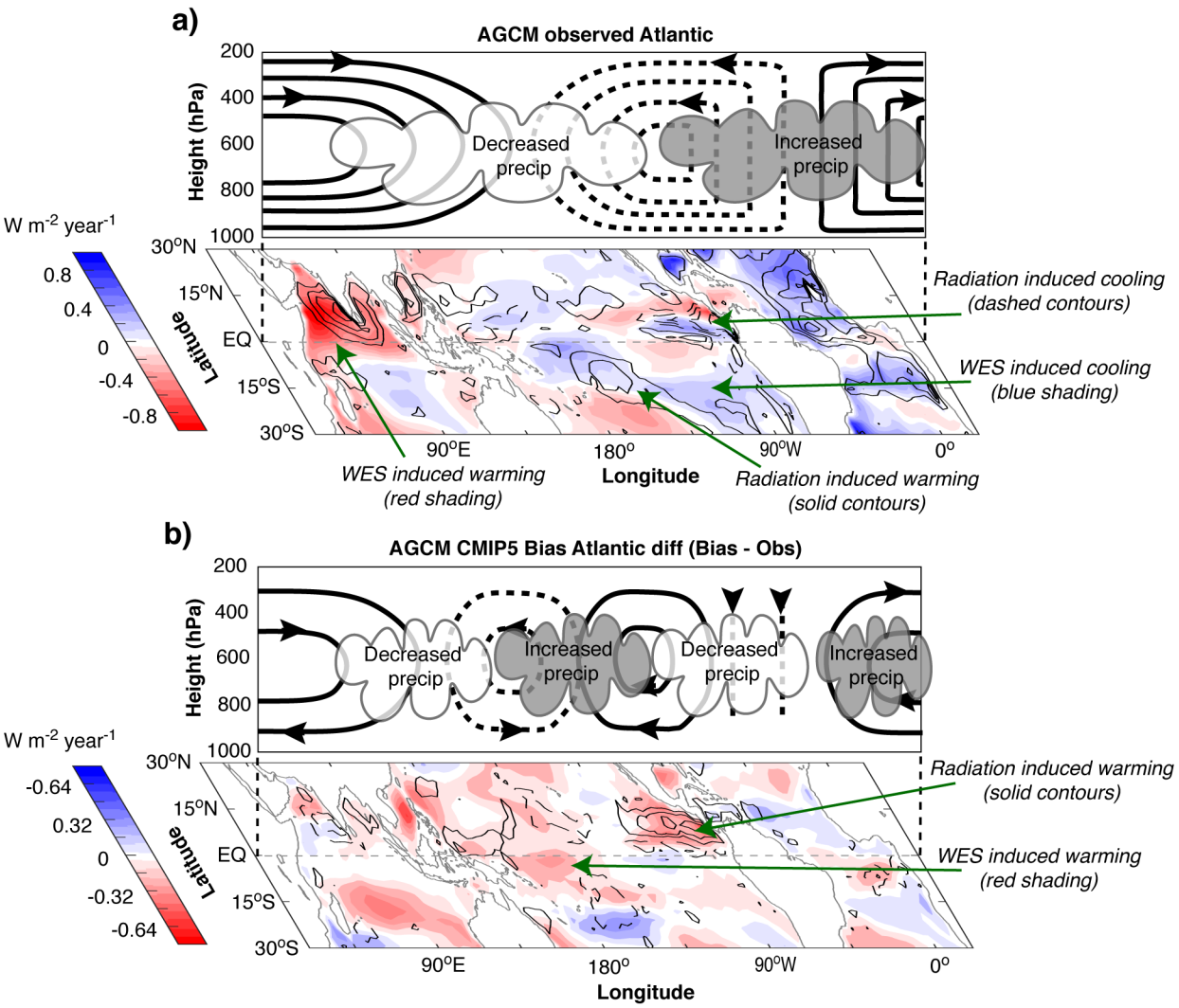

Figure 4: Schematic representation of the AGCM interbasin-link and the impact of the CMIP5 Atlantic SST bias. a, schematically represents the Atlantic SST trend induced changes in atmospheric circulation, along with the related modelled changes in surface radiation (contours) and latent heat flux (shading). B, schematically depicts the changes in atmospheric circulation from **a** due to the addition of CMIP5 Atlantic SST bias, while the related modelled changes from **a** in surface radiation (contours) and latent heat flux (shading).

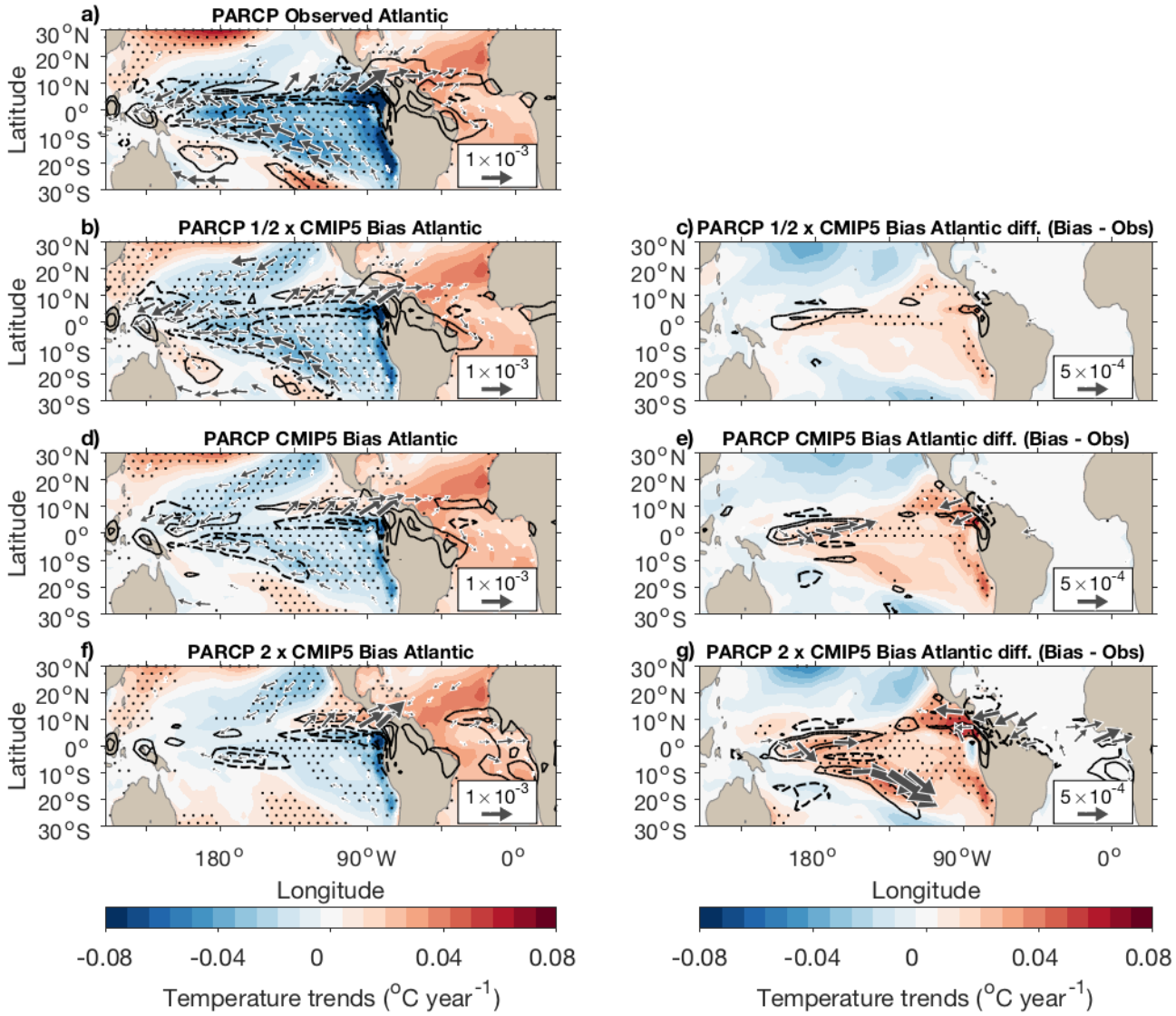

Figure 5: **Trends (1992–2011) of PARCP SST, wind stress and precipitation.**
a, Modelled surface temperature (shading, ^{o}C yr^{-1}), precipitation (contours; Pa yr^{-1}) and wind stress (vectors, N m^{-2} yr^{-1}) from the partially coupled experiment forced with observed Atlantic SST trend forcing, observed Atlantic background state and an active Pacific mixed layer; Stippling indicates that the temperature trends are significant above the 95% level, while only trends vectors that are significant above 95% level are plotted. Precipitation trend contours shown for 0.5 and 1 x10^{-9} m s^{-1} yr^{-1} in solid black, and corresponding negative trends in dashed black. **b, d,** & **f,** as in **a** but for the simulations with the CMIP5 biased Atlantic background state at half, full and double strength, respectively. **c**, **e** and **g** respectively presents the differences between **a** & **b**, **d** & **a**, and **f** & **a**. Stippling here indicates that there is no overlap between the 95% confidence intervals of the linear temperature trends of the two experiments differenced. Vectors are also only plotted when there is no overlap in the confidence intervals of the two differenced experiments. Precipitation trend difference contours shown for 2.5 and 5 x10^{-8} m s^{-1} yr^{-1} in solid black, and corresponding negative trends in dashed black.